Modeling visible and near-infrared snow surface reflectance-simulation and validation

Hongyi Wu (吴宏伊)* and Ling Tong (童 玲)

Institute of Geo-Spatial Information Science and Technology,
University of Electronic Science and Technology of China, Chengdu 611731, China
**Corresponding author: wuhongyi1008@163.com*

Received March 21, 2011; accepted April 28, 2011; posted online July 11, 2011

Retrieving snow surface reflectance is difficult in optical remote sensing. Hence, this letter evaluates five surface reflectance models, including the Ross-Li, Roujean, Walthall, modified Rahman and Staylor models, in terms of their capacities to capture snow reflectance signatures using ground measurements in Antarctica. The biases of all the models are less than 0.0003 in both visible and near-infrared regions. Moreover, with the exception of the Staylor model, all models have root-mean-square errors of around 0.02, indicating that they can simulate the reflectance magnitude well. The R^2 performances of the Ross-Li and Roujean models are higher than those of the others, indicating that these two models can capture the angle distribution of snow surface reflectance better.

OCIS codes: 290.0290, 300.0300, 330.0330, 280.0280, 350.0350.
doi: 10.3788/COL201109.102901.

The bidirectional reflectance distribution function (BRDF) characterizes the angular distribution of surface reflection[1,2]. It plays an important role in performing atmospheric correction, detecting land cover types, and calculating other biophysical parameters[3]. However, the retrieval of snow BRDF/albedo is always a difficult issue in the application of remotely sensed information. For pixel scale, existing satellite product validation systems have lower quality albedo/BRDF retrieval of snow surface compared with vegetation surface[4,5]. This phenomenon is due to two main reasons. First, the BRDF models used in the retrieval cannot present directional reflectance distribution over snow and vegetation[4]. Second, due to the high reflectance of both snow and cloud, it is more difficult to remove contamination from clouds in reflectance retrieval over snow than vegetation. We evaluate the simulation ability of snow surface reflectance of several current BRDF models by considering reports on the lower retrieval quality of BRDF/albedo over snow than vegetation. The simulation results provide comprehensive knowledge of snow surface reflectance in the hemisphere space. Models can also be selected according to the evaluation report. Finally, the quantified coefficients of models can serve as a background for future snow BRDF modeling projects.

Semi-empirical BRDF models describe the surface BRDF with linear or nonlinear form. Among these, the Ross-Li, Roujean, and modified Rahman models are used in current satellite albedo/BRDF algorithms. We chose them to fit the *in situ* measured snow surface reflectance data. The evaluation results can be used as feedback in future retrieval projects. The Walthall and Staylor models are also evaluated in this work. The Walthall model can easily fit in the algorithm due to its simple linear form. The Staylor model is generally formed for desert surfaces that are similar to the flat, optically thick snow medium[6].

The linear Ross–Li model is used in moderate-resolution imaging spectroradiometer (MODIS) albedo/BRDF products[7,8]. It can be expressed in Eq. (1) below:

$$R(\lambda,\theta_i,\theta) = f_{\rm iso}(\lambda)+f_{\rm vol}(\lambda)k_{\rm vol}(\theta_i,\theta)+f_{\rm geo}(\lambda)k_{\rm geo}(\theta_i,\theta), \quad (1)$$

where R is the surface bidirectional reflectance; θ_i and θ denote the illuminating and view directions, respectively; λ is the wavelength; and $f_{\rm iso}$, $f_{\rm vol}$, and $f_{\rm geo}$ are the three coefficients that have to be determined by fitting the observations, respectively. Detailed expressions of the two kernels $k_{\rm vol}$ and $k_{\rm geo}$ can be found in literature[9,10].

The modified Walthall model[11] is a four-coefficient (a, b, c, and d) linear model based on empirical considerations with the form:

$$R = a(\theta_i^2+\theta^2)+b\theta_i^2\theta^2+c\theta_i\theta\cos\varphi+d, \quad (2)$$

where φ is the relative azimuth angle.

The Roujean model[12] is a three-coefficient (k_0, k_1, and k_2) linear model used in the polarization and directionality of the earth's reflectances (POLDER) algorithm. Kernel f_1 estimates the reflectance of a flat surface, whereas f_2 attempts an approximation of the radiative transfer within a vegetation canopy, which is similar to Eq. (3) given by

$$R(\theta_i,\theta,\varphi) = k_0+k_1f_1(\theta_i,\theta,\varphi)+k_2f_2(\theta_i,\theta,\varphi). \quad (3)$$

The modified Rahman model[13] has been used in multi-angle imaging spectroradiometer (MISR) BRDF/albedo algorithm. It is a three-coefficient (r_0, k, and b) nonlinear model expressed as

$$R(-\mu,\mu_0,\varphi) = r_0[\mu_0\mu(\mu_0+\mu)]^{k-1} \cdot \exp[b\cdot p(\Omega)]\left(\frac{2+G-r_0}{1+G}\right), \quad (4)$$

where the Henyey–Greenstein function $p(\Omega)$ accounts for the phase function of scattering elements, and $\frac{2+G-r_0}{1+G}$ explicitly accounts for the hot spot, $\mu=\cos(\theta)$, and

$\mu_i = \cos(\theta_i)$.

Both snow and desert are regarded as flat, optically thick media because of the weak absorption caused by more scattering events internal to the media[6]. Hence, we tried Staylor model with four coefficients (c_1, c_2, c_3, and N)[14] to evaluate its capability in capturing snow BRDF using the expression below:

$$R(\theta_i, \theta, \varphi) = \frac{1/\mu\mu_i[c_1 + c_2([\mu\mu_i/\mu + \mu_i])^N]}{2\int_0^1 B(\mu, \mu_i)\mu_i \mathrm{d}\mu} \cdot \frac{1 + c_3(\mu\mu_i - \sin\theta_i \sin\theta \cos\varphi)^2}{1 + c_3[(\mu\mu_i)^2 + (1/2)(\sin\theta_i \sin\theta)^2]}. \quad (5)$$

In situ measurements were used to evaluate models because they provide the most direct observations of surface BRDF[15]. A ground measured data set provided by solar radiation processes on the East Antarctic Plateau was used to fit these models[16]. The measurements were performed using a field-spec pro JR spectroradiometer manufactured by Analytical Spectral Devices, Inc. (ASD)[17]. This data set had *in situ* measurements of snow surface reflectance covering a wavelength ranging from 350 to 2 400 nm.

We chose *in situ* data of 450, 550, 650, and 850 nm for the simulations because most satellite databases provided BRDF and albedo products in blue, green, red, and near-infrared (NIR) bands. We used such data to produce broadband albedo products. In each band, we observed the azimuth angle every 15° from 0° to 180°; we also viewed the zenith angle every 15° from 7.5° to 82.5°. Figure 1 shows the example of snow surface reflectance in four bands with solar zenith angle of 56°. The chosen data were fitted with the selected models using the SCE-UA optimal method[18] in order to minimize the root-mean-square error (RMSE) between the outputs of the models and the measurements.

We did not compare the simulation results and measurements with view angles larger than 80° in subsequent analyses. This is due to the lack of ground measurements with view zenith angle over 82.5°, and because BRDF inversion in remote sensing does not involve observations in large view angles.

Figure 2 represents the simulation results for ground measurements in four bands. Outputs from every model captured the high reflection of snow in the forward direction. Compared with those in Fig. 1, outputs from the Ross-Li and Roujean models are close to the ground measurements in the hemisphere region. However, for the large view zenith angle (viewing close to horizontal, that is, the external circle in every figure in Fig. 2), these two models have obvious negative biases. Moreover, the Rahman and Staylor models have extreme positive biases for the large view zenith angle.

As the quantitative modeling results, all the coefficients of the models are listed in Table 1 for future snow BRDF simulations. Table 1 also present comparisons between the fitting results and the measurements from the four bands, respectively. The RMSE and R^2 performances of all the models are better fitted than the satellite snow BRDF signatures reported in previous literature[3,4]. However, the performances of the Ross-Li, Rahman, Roujean, and Walthall models differ slightly.

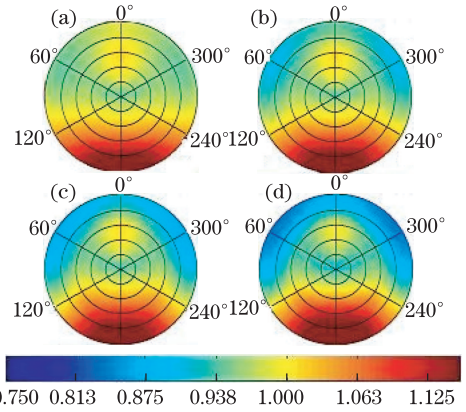

Fig. 1. Ground measurements of snow surface reflectance. (a)–(d): Wavelengths of 450, 550, 650, and 850 nm. The polar angle represents the relative azimuth angle. Radii of the circles (1, 0.8, 0.6, 0.4, and 0.2) indicate the projection of view direction: radius= $1 - \cos(\theta)$.

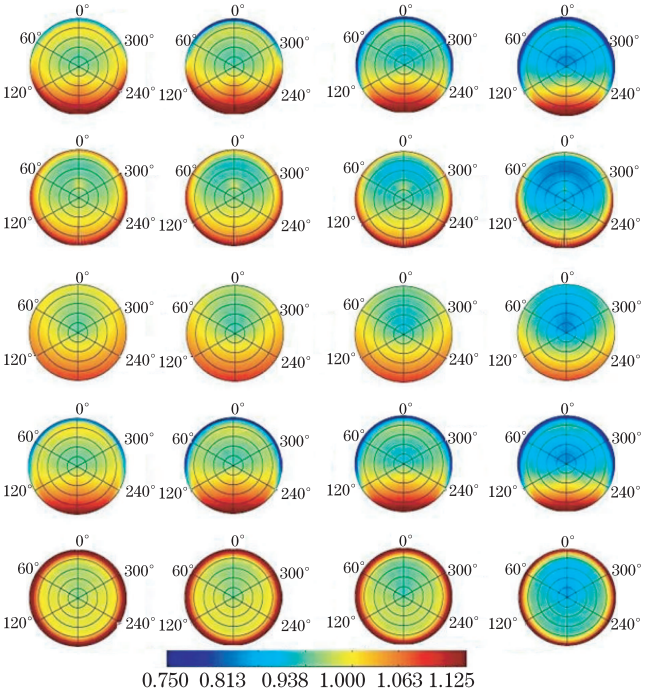

Fig. 2. Model simulations of snow surface reflectance. First line to the last: outputs from the Ross-Li, Rahman, Walthall, Roujean, and Staylor models. First column to the last: wavelengths of 450, 550, 650, and 850 nm.

The bias performances of all models are less than 0.0003 in both visible and NIR regions. With the exception of the Staylor model, all the models have RMSE values of around 0.02, indicating that they can simulate the reflectance magnitude well. The R^2 performances of the Ross-Li and Roujean models are between 0.73–0.76 in the visible bands, and are over 0.81 in the NIR band. The high relation coefficients indicate that these two models capture the angle distribution of snow surface reflectance better than the other models.

The ground measurements we used in the present work have abundant and well-distributed BRDF samplings. In this condition, all five models showed high capability in simulating snow surface reflectance. However, remote

Table 1. Quantified Coefficients of Models and Comparisons between Ground Measurements and Model Outputs for Wavelengths of 450, 550, 650, and 850 nm

Wavelength (nm)	Model	Quantified Coefficients	Bias	RMSE	R^2
450	Ross-Li	$f_{\rm iso}$=0.9700, $f_{\rm vol}$=0.0998, $f_{\rm geo}$=0.0095	0.0001	0.0224	0.8124
	Rahman	r_0=0.8480, k=0.9352, b=0.0824	−0.0004	0.0187	0.7092
	Walthall	a=−0.050, b=0.0912, c=0.0335, d=1.0000	−0.0001	0.0222	0.5872
	Roujean	k_0=0.9719, k_1=0.0144, k_2=0.2470	0.0000	0.0174	0.7477
	Staylor	c_1=0.0996, c_2=8.2805, c_3=−0.024, N=2.8874	0.0000	0.0423	0.3295
550	Ross-Li	$f_{\rm iso}$=0.9726, $f_{\rm vol}$=0.1015, $f_{\rm geo}$=0.0146	0.0001	0.0203	0.7351
	Rahman	r_0=0.8314, k=0.9310, b=0.0981	−0.0005	0.0216	0.7020
	Walthall	a=−0.054, b=0.0942, c=0.0417, d=0.9999	0.0000	0.0256	0.5802
	Roujean	k_0=0.9746, k_1=0.0217, k_2=0.2602	0.0000	0.0197	0.7519
	Staylor	c_1=0.0965, c_2=8.0117, c_3=−0.032, N=2.8538	−0.0003	0.0344	0.2421
650	Ross-Li	$f_{\rm iso}$=0.9580, $f_{\rm vol}$=0.1093, $f_{\rm geo}$=0.0166	−0.0001	0.0214	0.7512
	Rahman	r_0=0.7990, k=0.9226, b=0.1122	−0.0004	0.0225	0.7249
	Walthall	a=−0.072, b=0.1159, c=0.0465, d=0.9999	0.0000	0.0271	0.6005
	Roujean	k_0=0.9605, k_1=0.0246, k_2=0.2818	0.0000	0.0206	0.7655
	Staylor	c_1=0.0959, c_2=7.8137, c_3=−0.039, N=2.8494	0.0000	0.0370	0.2541
850	Ross-Li	$f_{\rm iso}$=0.9010, $f_{\rm vol}$=0.1094, $f_{\rm geo}$=0.0188	0.0001	0.0224	0.8124
	Rahman	r_0=0.7001, k=0.8914, b=0.1506	−0.0004	0.0187	0.7092
	Walthall	a=−0.138, b=0.2010, c=0.0572, d=0.9999	−0.0001	0.0222	0.5872
	Roujean	k_0=0.9030, k_1=0.0275, k_2=0.3677	0.0000	0.0174	0.7477
	Staylor	c_1=0.0883, c_2=6.4735, c_3=−0.053, N =2.7315	0.0000	0.0423	0.3298

sensors had difficulty in providing abundant angular samplings as well as those with a high viewing resolution. For homogenous surfaces, such as pure snow, a combination of observations from various sensors can provide more surface reflectance samplings, resulting in better retrieval quality.

This work was supported by the National "863" Program of China (No. 2009AA122101) and the National Natural Science Foundation of China (Nos. 40871160 and 60841006).

References

1. S. Liang, *Quantitative Remote Sensing of Land Surfaces* (Hoboken, Wiley-IEEE, 2004).
2. W. Zhang, H. Wang, and Z. Wang, Chin. Opt. Lett. **7,** 88 (2009).
3. F. Maignan, F.-M. Breon, and R. Lacaze, Remote Sens. Environ. **90,** 210 (2004).
4. P. Bicheron and M. Leroy, J. Geophys. Res. **105,** 26669 (2000).
5. Y.-M. Chen, S. Liang, J. Wang, H.-Y. Kim, and J. V. Martonchik, Int. J. Remote Sens. **29,** 6971 (2008).
6. M. I. Mishchenko, J. M. Dlugach, E. G Yanovitskij, and N. T. Zakharova, J. Quant. Spectrosc. Ra. **63,** 409 (1999).
7. Y. Jin, F. Gao, C. B. Schaaf, X. Li, A. H. Strahler, C. J. Bruegge, and J. V. Martonchik, IEEE Trans. Geosci. Remote Sens. **40,** 1593 (2002).
8. W. Lucht, C. B. Schaaf, and A. H. Strahler, IEEE Trans. Geosci. Remote Sens. **38,** 977 (2000).
9. X. Li and A. H. Strahler, IEEE Trans. Geosci. Remote Sens. **30,** 276 (1992).
10. W. Wanner, X. Li, and A. H. Strahler, J. Geophys. Res. **100,** 21077 (1995).
11. C. L. Walthall, J. M. Norman, J. M. Welles, G. Campbell, and B. L. Blad, Appl. Opt. **24,** 383 (1985).
12. J. L. Roujean, M. Leroy, and P. Y. Deschamps, J. Geophys. Res. **97,** 20455 (1992).
13. H. Rahman, M. M. Verstraete, and B. Pinty, J. Geophys. Res. **98,** 20779 (1993).
14. W. F. Staylor and J. T. Suttles, J. Climate Appl. Meteorol. **25,** 196 (1985).
15. Z. Zhao, C. Qi, and J. Dai, Chin. Opt. Lett. **5,** 168 (2007).
16. S. R. Hudson, S. G. Warren, R. E. Brandt, T. C. Grenfell, and D. Six, J. Geophys. Res. **111,** D18106 (2006).
17. B. C. Kindel, Z. Qu, and A. F. H. Goetz, Appl. Opt. **40,** 3483 (2001).
18. Q. Duan, S. Sorooshian, and V. Gupta, Water Resour. Res. **28,** 1015 (1992).